

Rapid 3D μ -printing of polymer optical whispering-gallery mode resonators

Jushuai Wu,¹ Xin Guo,^{1,2} A. Ping Zhang,^{1,*} and Hwa-Yaw Tam¹

¹Photonics Research Centre, Department of Electrical Engineering, The Hong Kong Polytechnic University, Kowloon, Hong Kong SAR, China

²State Key Laboratory of Modern Optical Instrumentation, College of Optical Science and Engineering, Zhejiang University, Hangzhou, Zhejiang 310027, China

*azhang@polyu.edu.hk

Abstract: A novel microfabrication method for rapid printing of polymer optical whispering-gallery mode (WGM) resonators is presented. A 3D micro-printing technology based on high-speed optical spatial modulator (SLM) and high-power UV light source is developed to fabricate suspended-disk WGM resonator array using SU-8 photoresist. The optical spectral responses of the fabricated polymer WGM resonators were measured with a biconically tapered optical fiber. Experimental results reveal that the demonstrated method is very flexible and time-saving for rapid fabrication of complex polymer WGM resonators.

©2015 Optical Society of America

OCIS codes: (120.4610) Optical fabrication; (220.3740) Lithography; (230.5750) Resonators.

References and links

1. K. J. Vahala, "Optical microcavities," *Nature* **424**(6950), 839–846 (2003).
2. S. C. Yang, Y. Wang, and H. D. Sun, "Advances and prospects for whispering gallery mode microcavities," *Adv. Opt. Mater.* **3**(9), 1136–1162 (2015).
3. D. Keng, X. Tan, and S. Arnold, "Whispering gallery micro-global positioning system for nanoparticle sizing in real time," *Appl. Phys. Lett.* **105**(7), 071105 (2014).
4. V. R. Dantham, S. Holler, V. Kolchenko, Z. Wan, and S. Arnold, "Taking whispering gallery-mode single virus detection and sizing to the limit," *Appl. Phys. Lett.* **101**(4), 043704 (2012).
5. F. Vollmer and S. Arnold, "Whispering-gallery-mode biosensing: label-free detection down to single molecules," *Nat. Methods* **5**(7), 591–596 (2008).
6. M. R. Foreman, J. D. Swaim, and F. Vollmer, "Whispering gallery mode sensors," *Adv. Opt. Photonics* **7**(2), 168–240 (2015).
7. Q. Ma, L. Huang, Z. Guo, and T. Rossmann, "Spectral shift response of optical whispering-gallery modes due to water vapor adsorption and desorption," *Meas. Sci. Technol.* **21**(11), 115206 (2010).
8. F. Sedlmeir, R. Zeltner, G. Leuchs, and H. G. L. Schwefel, "High-Q MgF₂ whispering gallery mode resonators for refractometric sensing in aqueous environment," *Opt. Express* **22**(25), 30934–30942 (2014).
9. M. Eryürek, Y. Karadag, N. Taştaltın, N. Kılınc, and A. Kiraz, "Optical sensor for hydrogen gas based on a palladium-coated polymer microresonator," *Sens. Actuat. B Chem.* **212**, 78–83 (2015).
10. D. K. Armani, T. J. Kippenberg, S. M. Spillane, and K. J. Vahala, "Ultra-high-Q toroid microcavity on a chip," *Nature* **421**(6926), 925–928 (2003).
11. A. Matsko and V. Ilchenko, "Optical resonators with whispering-gallery modes-part I: basics," *IEEE J. Sel. Top. Quantum Electron.* **12**(1), 3–14 (2006).
12. T. J. Kippenberg, S. M. Spillane, D. K. Armani, and K. J. Vahala, "Ultralow-threshold microcavity Raman laser on a microelectronic chip," *Opt. Lett.* **29**(11), 1224–1226 (2004).
13. M. C. Collodo, F. Sedlmeir, B. Sprenger, S. Svitlov, L. J. Wang, and H. G. L. Schwefel, "Sub-kHz lasing of a CaF₂ whispering gallery mode resonator stabilized fiber ring laser," *Opt. Express* **22**(16), 19277–19283 (2014).
14. V. S. Ilchenko, A. A. Savchenkov, A. B. Matsko, and L. Maleki, "Nonlinear optics and crystalline whispering gallery mode cavities," *Phys. Rev. Lett.* **92**(4), 043903 (2004).
15. A. Schliesser and T. J. Kippenberg, "Cavity optomechanics with whispering-gallery mode optical micro-resonators," *Adv. At. Mol. Opt. Phys.* **58**, 207–323 (2010).
16. H. Lee, T. Chen, J. Li, K. Y. Yang, S. Jeon, O. Painter, and K. J. Vahala, "Chemically etched ultrahigh-Q wedge-resonator on a silicon chip," *Nat. Photonics* **6**(6), 369–373 (2012).
17. P. Rabiei, W. H. Steier, C. Zhang, and L. R. Dalton, "Polymer micro-ring filters and modulators," *J. Lightwave Technol.* **20**(11), 1968–1975 (2002).
18. A. L. Martin, D. K. Armani, L. Yang, and K. J. Vahala, "Replica-molded high-Q polymer microresonators," *Opt. Lett.* **29**(6), 533–535 (2004).
19. T. Grossmann, M. Hauser, T. Beck, C. Gohn-Kreuz, M. Karl, H. Kalt, C. Vannahme, and T. Mappes, "High-Q conical polymeric microcavities," *Appl. Phys. Lett.* **96**(1), 013303 (2010).

20. A. P. Zhang, X. Qu, P. Soman, K. C. Hribar, J. W. Lee, S. Chen, and S. He, "Rapid fabrication of complex 3D extracellular microenvironments by dynamic optical projection stereolithography," *Adv. Mater.* **24**(31), 4266–4270 (2012).
21. A. N. Oraevsky, "Whispering-gallery waves," *Quantum Electron.* **32**(5), 377–400 (2002).
22. H. G. L. Schwefel, A. D. Stone, and H. E. Tureci, "Polarization properties and dispersion relations for spiral resonances of a dielectric rod," *J. Opt. Soc. Am. B* **22**(11), 2295–2307 (2005).
23. M. Oxborrow, "Traceable 2-D finite element simulation of the whispering gallery modes of axisymmetric electromagnetic resonators," *IEEE Trans. Microw. Theory Tech.* **55**(6), 1209–1218 (2007).
24. A. Borreman, S. Musa, A. A. M. Kok, M. B. J. Diemeer, and A. Driessen, "Fabrication of polymeric multimode waveguides and devices in SU-8 photoresist using selective polymerization," in *IEEE/LEOS Benelux Chapter 2002 Annual Symposium*, (IEEE, 2002), pp. 83–86.
25. M. L. Gorodetsky, A. A. Savchenkov, and V. S. Ilchenko, "Ultimate Q of optical microsphere resonators," *Opt. Lett.* **21**(7), 453–455 (1996).
26. I. Breunig, B. Sturman, F. Sedlmeir, H. G. L. Schwefel, and K. Buse, "Whispering gallery modes at the rim of an axisymmetric optical resonator: analytical versus numerical description and comparison with experiment," *Opt. Express* **21**(25), 30683–30692 (2013).
27. M. Nordström, D. A. Zauner, A. Boisen, and J. Hübner, "Single-mode waveguides with SU-8 polymer core and cladding for MOEMS applications," *J. Lightwave Technol.* **25**(5), 1284–1289 (2007).

1. Introduction

Optical whispering-gallery modes (WGM) are distinct resonances of an optical field confined near the surface of a special resonator by total internal reflection [1,2]. The spectral responses of optical WGM resonators greatly rely on the device geometry. As their evanescent fields extending to surrounding environment are greatly sensitive to external perturbations, the induced shift or broadening of the resonant peaks can be utilized for ultrasensitive sensing, e.g. the detection of single particle or virus [3–5], and the sensing of vapor or hydrogen gas [6–9]. Moreover, owing to the low scattering loss and small mode volume, optical WGM resonators can usually attain ultra-high quality (Q) factors and high optical density [10,11]. Such unique optical properties make WGM resonators an ideal platform to exploit emerging photonic phenomena and devices from low-threshold lasing [12, 13] and nonlinear optics [14] to cavity optomechanics [15].

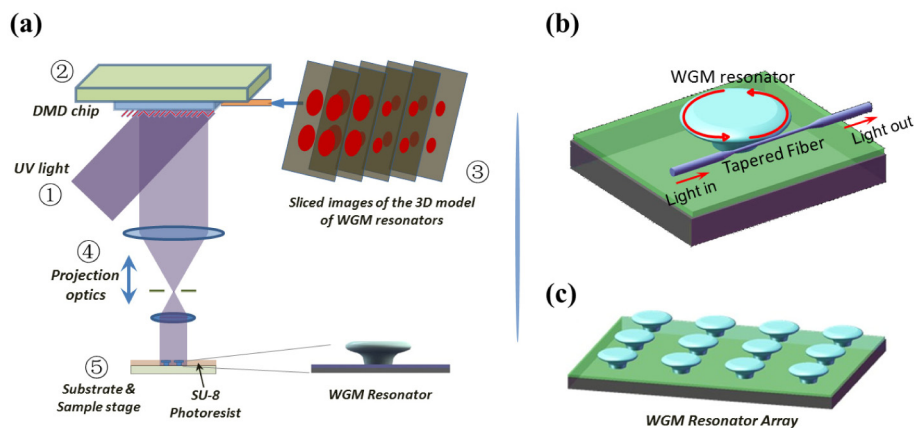


Fig. 1. (a) Schematic diagram of the 3D μ Printing technology: UV light illuminates the DMD chip, which reflects light patterns according to the images sliced from a 3D model of suspended-disk WGM resonator. The polymer WGM resonator is fabricated by using a layer-by-layer polymerization process; (b) light coupling between a WGM resonator and tapered optical fiber; (c) WGM resonator array.

In order to develop new devices based on optical WGM resonators, one needs a feasible approach to fabricate high-quality WGM resonators. The commonly used fabrication method for nonspherical optical WGM resonators contains four steps: photolithography, pattern transfer, selective etching of exposed substrates, and selective reflow of patterned structures [10, 16]. These processes are rather time-consuming and might limit their practical applications, particularly for cost-sensitive devices. The issue mentioned above can be solved

by using polymer optical WGM microresonators [17–19]. Compared with microresonators fabricated in inorganic materials, polymer WGM resonators have the advantages of biocompatibility, low cost, and ease of fabrication. For instance, a replica-molding method was demonstrated to fabricate toroid-shape polydimethylsiloxane (PDMS) WGM resonators [18]. Although the demonstrated method is a very fast and effective approach to produce PDMS WGM resonators and even dense arrays of devices, the technique is still a material- and shape- dependent process.

In this paper, we demonstrate a novel optical microfabrication method, as illustrated in Fig. 1, to rapidly fabricate optical WGM resonators and resonator array in photoresist. Figure 1(a) shows the optical 3D micro-printing setup where a high-power UV light source (OmniCure 2000 System, Lumen Dynamic Group Inc.) and a high-speed spatial-light modulator, i.e. digital micromirror device (DMD, DLi4120 0.7" XGA, Texas Instruments), are used to construct an optical maskless stereolithography system. Owing to the dynamic pattern generation capability of the DMD chip, the UV light reflected by the DMD chip creates 2D optical patterns according to the images sliced from a 3D model of the WGM resonator. After passing through projection optics, the optical patterns are projected upon the photoresist which was spin-coated on a substrate. Based on the monotonically additive light-absorption property of the photoresist, a predefined polymer WGM resonator can be fabricated in a layer-by-layer polymerization manner [20]. Compared with previously reported fabrication approaches [10,16–19], this 3D micro-printing technology is much more flexible for fabrication of complex WGM resonators. It is particularly suitable for direct printing of polymer WGM resonators for on-chip integration in real-world applications.

2. Fabrication and simulation

In the experiment, a common epoxy-based negative photoresist SU-8 was used to fabricate polymer WGM resonators. It has good optical property (highly transparent in both visible and near infrared band range) and also excellent chemical resistance and mechanical property, and thus is well-suited material for optical micro/nano-devices. The SU-8 photoresist used in the experiments is EPON resin SU-8 (Momentive Ltd). Octoxyphenylphenyliodonium hexafluoroantimonate (OPPI) (Hampford Research Inc.) and tributylamine (Merck Chemical Technology Co., Ltd.) were used as photoacid generator and inhibitor, respectively. These compositions were dissolved by using cyclopentanone in a weight ratio of OPPI/tributylamine/SU-8 = 2:0.014:100. In order to improve the adhesion between SU-8 photoresist and glass substrate, a SU-8 buffer layer with thickness of around 2 μm was fabricated before 3D micro-printing processes. Thereafter, a 100 μm thick SU-8 photoresist was spin-coated on the top of the buffer layer. The sample was then soft baked at 65 $^{\circ}\text{C}$ for 7 minutes and 95 $^{\circ}\text{C}$ for 20 minutes to remove the solvent.

A dynamic optical exposure equipment, as shown in Fig. 1(a), was then developed to expose the SU-8 photoresist by using a dynamic image projection scheme. In order to fabricate a predefined WGM resonator, its 3D model was designed by using a commercial CAD software. An own-developed add-on software was used to slice the 3D model into 200 layers to generate a series of image data. These images were then sequentially loaded to the DMD chip to dynamically generate predefined light patterns. 3D microstructures were fabricated owing to the additive penetration depth of light on the photoresist. Both the projection optics and the substrate kept motionless during the exposure process. The light intensity of the UV light used in the exposure process was 104.85 mW/cm^2 . The exposed time of each layer of the 3D model was calibrated according to the relationship between the exposed time and cured thickness of SU-8 photoresist. The expose time for each layer was 275 milliseconds, and the total expose time was 55 seconds. After the exposure process, the sample was post-baked on a hot plate at 65 $^{\circ}\text{C}$ for 5 minutes and 95 $^{\circ}\text{C}$ for 10 minutes and developed in propyleneglycol monomethylether acetate (PGMEA) for 6 minutes.

Figure 2(a) shows an optical microscope image of the fabricated SU-8 WGM resonators, and Figs. 2(b) and 2(c) are the scanning electron microscope (SEM) images of the WGM resonators. One can see that the suspended-disk WGM resonators, directly printed on the

substrate by using a one-step optical exposure process, have very smooth surface. The root-mean-square roughness is about 5.11 nm, which was measured by using an atomic force microscope (MultiMode 8, Bruker, Germany). The geometry of the fabricated WGM resonator is almost the same as the designed one shown in Fig. 1(b). The outer diameter of the suspended-disk of the WGM resonators is 460 μm , and the height of the whole WGM resonator is about 100 μm . Figure 1(c) shows the SEM image of an array of SU-8 WGM resonators fabricated by the one-step exposure process. The results reveal that the fabrication process is very flexible and capable for rapid large-scale production of WGM resonators. It should be noted that the demonstrated process is not material specific and can be applied to most photo-crosslinkable polymeric materials.

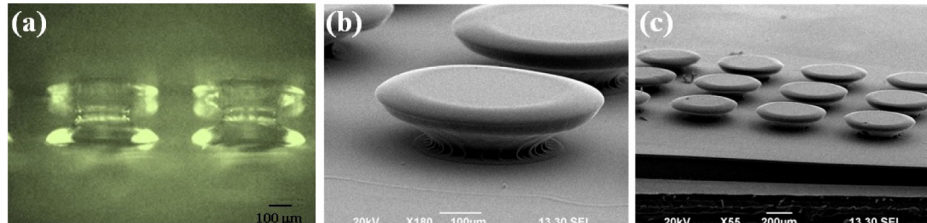


Fig. 2. Microscope images of the fabricated SU-8 suspended-disk WGM resonators: (a) optical microscope image of the fabricated WGM resonators and its mirror image in the side view, (b) SEM image of a WGM resonator, and (c) SEM image of WGM resonator array.

Using the measured geometric parameters, numerical simulations were conducted to reveal the optical field distribution and spectral characteristics of the suspended-disk WGM resonators. Finite element method (FEM) for open axisymmetric resonators (without invoking any transverse mode approximation to Maxwell's equations) of the simulation package COMSOL Multiphysics was used to simulate the possible resonant modes and their spatial distributions. Rotational symmetry of the device was used to reduce memory for the simulation [21–23]. Therefore, a 2D cylindrical coordinate system was used to solve Maxwell's equations.

The mode structure of the suspended-disk WGM resonator can be characterized by four indices (p, q, m, l), where p denotes the polarization of its electromagnetic field (TE or TM polarization); q is the radial order number denoting the number of maxima in the radial direction; m is the azimuthal mode number denoting the number of maxima in the equatorial plane; l is the polar mode number denoting the number of wavelengths packed along the circumference of the resonators. Figure 3(a) shows the model of the suspended-disk WGM resonator, and Figs. 3(b)-3(e) show the calculated intensity distributions of three typical resonance modes of the device at the wavelength of 1500.412 nm, 1495.568 nm and 1490.994 nm, respectively. Simulation results reveal that the optical field of its fundamental TE mode has 1490 maximas in equatorial plane, and its evanescent field leaking from the device to free space is around 0.062% energy of the entire mode.

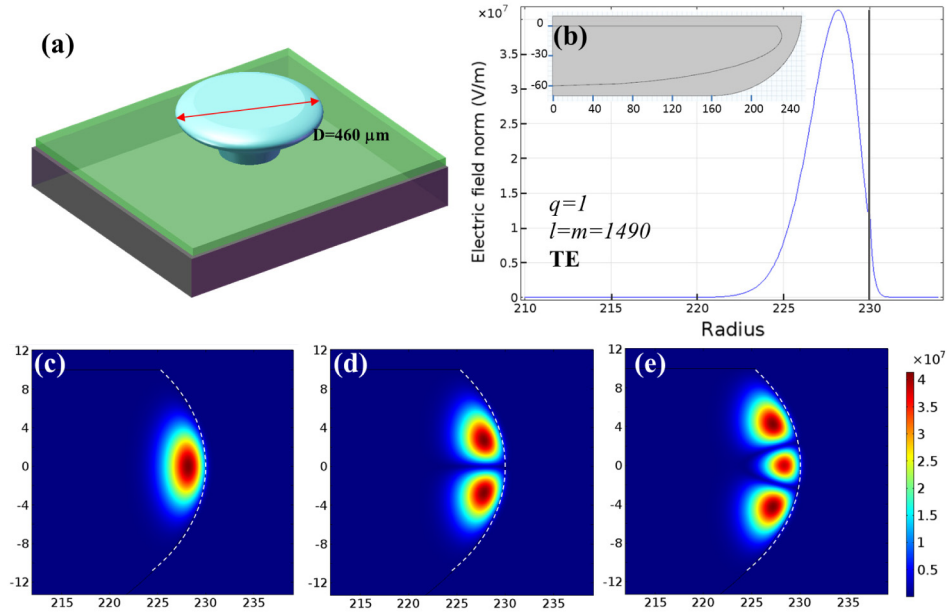


Fig. 3. (a) Schematic of a suspended-disk SU-8 WGM resonator with the diameter of 460 μm ; (b) The radial field distribution of its fundamental mode; (c), (d), and (e) are the field distributions of WGMs at the cross section of the device. The characteristic indices $(q, m, l) = (1, 1490, 1490)$, $(1, 1490, 1491)$ and $(1, 1490, 1492)$, respectively.

3. Spectrum measurement

In order to optically characterize the fabricated SU-8 WGM resonator, a biconically tapered optical fiber with waist diameter of about 2 μm was prepared to couple light in the resonator's equatorial plane. The fiber was attached to a 5-axis translation stage which allows precise positioning of the tapered fiber to approach the resonator. Two CCD cameras were used to monitor their relative positions from both top and side. In order to determine the best relative-position for excitation of WGM resonances, a 650-nm-wavelength laser beam was initially launched into the fiber for assistance of the alignment. Figures 4(a) and 4(b) show the optical microscope images of a SU-8 WGM resonator and the tapered optical fiber under test. After carefully adjusting the relative position between the tapered optical fiber and the device,

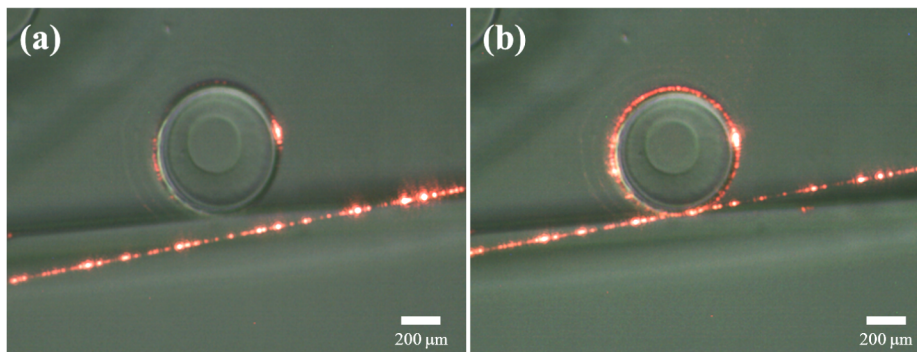


Fig. 4. Optical microscope images of a SU-8 WGM resonator coupling with a tapered optical fiber: (a) the tapered optical fiber is out of coupled regime; (b) the tapered optical fiber is within coupled regime. A 650-nm-wavelength laser beam was launched into the fiber for observation.

one can see that WGMs can be efficiently excited by using the tapered fiber based light coupling setup.

After elaborate alignment, a broadband light source in the optical telecommunication band (around 1500 nm) and an optical spectrum analyzer (OSA) with a resolution of 0.02 nm were then used to measure the transmission spectra of the WGM resonator. Figure 5 shows two measured transmission spectra of two SU-8 WGM resonators with the radiuses of 230 μm and 160 μm , respectively. One can see that WGM resonant frequencies can be clearly observed in the measured transmission spectra. The full-width at half-maximums (FWHMs) of the WGM resonant peaks of the two devices are 0.23 and 0.31 nm, and their averaged free-spectral ranges (FSRs) are 1.00 and 1.44 nm, respectively. They are in good agreement with the theoretical values 1.01 and 1.47 nm which are calculated by

$$\Delta\lambda_{\text{FSR}} \approx \lambda^2 / (2\pi nR), \quad (1)$$

where the refractive index of SU-8 photoresist around 1500 nm is $n = 1.57$ [24]. Those subsidiary peaks appearing in the transmission spectra are caused by high-order radial and azimuthal modes of the WGM resonator, which were also predicted by the simulation results.

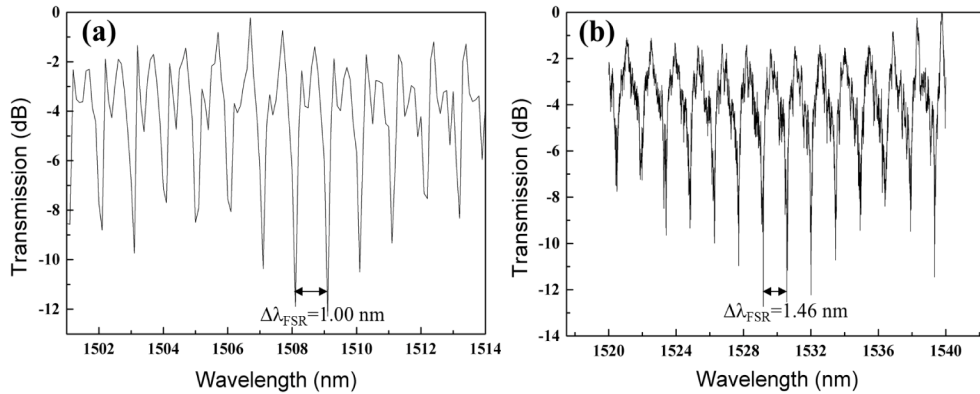


Fig. 5. Transmission spectra of the SU-8 WGM resonators with the radiuses of (a) 230 μm and (b) 160 μm . Additional subsidiary peaks are attributed to other radial or azimuthal modes.

The quality factor (Q) of a WGM resonator is defined as:

$$Q \approx \frac{\omega}{\Delta\omega_{\text{FWHM}}} \approx \frac{\lambda}{\Delta\lambda_{\text{FWHM}}} \quad (2)$$

where ω and λ is the central angular frequency and wavelength of the measured resonance, and $\Delta\omega_{\text{FWHM}}$ and $\Delta\lambda_{\text{FWHM}}$ is the FWHM of the lorentzian-shaped resonance. According to the measured FWHMs of the two resonators, the Q -factors of the two SU-8 WGM resonators are 6.4×10^3 and 4.9×10^3 , respectively.

4. Discussion and conclusion

Compared with some high-quality WGM resonators, the measured Q factors of the fabricated SU-8 WGM resonators are not high. The low- Q factor might be caused by: 1) relatively low resolution of the spectrum analyzer equipped in our lab. The optical resolution of the spectrum analyzer is 0.02 nm which is around one twelfth of the FWHMs of the WGM resonant peaks. Although it can marginally resolve the transmission spectra of the fabricated WGM resonators, a higher-resolution spectrum measurement instrument (e.g. a tunable laser based spectrum measurement setup) can more precisely reveal the profile of resonant peaks; 2) the own-fabricated tapered optical fiber and the light coupling setup might be not perfect. As the refractive index discrepancy between the silica optical fiber and SU-8 photoresists are considerable significant, the mode matching between the tapered optical fiber and the

polymer WGM resonators might be inefficient. Such a mode mismatching will cause a certain amount of loss and then degrade the dynamic ranges of resonant peaks [11]; 3) surface scattering induced by the roughness and contaminants. Besides the measurement errors, the most significant sources of Q-factor degradation of WGM resonators are known as material absorption and surface scattering [25, 26]. Since the absorption coefficient of the cured SU-8 photoresist at the wavelength around 1500 nm is around 2.0 dB/cm [27], the material-absorption limited Q value can be estimated as 1.43×10^5 . Therefore, it is believed that the Q-factor can be further enhanced through improvement of surface smoothness and the depression of contamination. The surface smoothness can be improved by using a higher demagnification projection optics and fabrication parameter optimization, and the contamination issue can be solved if the whole fabrication and coupling processes are conducted in a clean environment.

In conclusion, we have presented a 3D micro-printing method to rapidly fabricate polymer optical WGM resonators. It has been demonstrated the technology can rapidly fabricate SU-8 suspended-disk optical WGM resonators and resonator array. The transmission spectra of the optical WGM resonators were measured, which are in good agreement with theoretical predictions. The proposed 3D micro-printing technology is not a material dependent approach and thus is very promising to rapidly fabricate various polymer optical WGM resonators for the development of versatile and compact photonic devices.

Acknowledgments

This work was partially supported by Hong Kong RGC GRF (Grant No.: PolyU 152211/14E) and PolyU Departmental General Research Fund (Grant No.: 4-ZZBE).